# Number-conserving approach to the pairing problem: Application to Kr and Sn isotopic chains

Guillaume Hupin[1,2,*] and Denis Lacroix[1,†]

[1]*Grand Accélérateur National d'Ions Lourds (GANIL), CEA/DSM-CNRS/IN2P3, Boulevard Henri Becquerel, 14076 Caen, France*

[2]*Lawrence Livermore National Laboratory, P.O. Box 808, L-414, Livermore, California 94551, USA*

(Received 2 May 2012; revised manuscript received 7 July 2012; published 17 August 2012)

The recently proposed symmetry-conserving energy density functional approach [G. Hupin, D. Lacroix, and M. Bender, Phys. Rev. C **84**, 014309 (2011)] is applied to perform variation after projection onto the good particle number using the Skyrme interaction, including density-dependent terms. We propose a simplification to reduce the numerical effort to perform the variation. We present a systematic study of the Kr and Sn isotopic chains. This approach leads to nonzero pairing in magic nuclei and a global enhancement of the pairing gap compared to the original theory, which breaks particle number symmetry.

DOI: 10.1103/PhysRevC.86.024309 PACS number(s): 21.60.Jz, 71.15.Mb, 74.20.−z, 74.78.Na

## I. INTRODUCTION

The nuclear energy density functional (EDF) is a versatile approach [1,2] that allows one to describe a variety of phenomena in nuclei ranging from nuclear structure effects to nuclear dynamics and to thermodynamics. One specificity of nuclear energy functional approaches is that the densities used in the energy might not respect some of the properties related to the symmetry of the underlying bare many-body Hamiltonian [3,4]. This is achieved by introducing a reference Slater (or quasiparticle) state from which the one-body normal density (and eventually the anomalous density) is constructed to express the energy. These densities are generally localized in space and therefore do not correspond to a translationally invariant system. Symmetry breaking is often extended to states that are neither an eigenstate of the particle number operator [then breaking U(1) symmetry] nor an eigenstate of the total angular momentum operator.

Symmetry-breaking EDF (SB-EDF) is a powerful technique to describe some aspects of nuclei such as the onset of pairing and/or deformation. First, however, restoration of broken symmetries is necessary to compare with experiment, where eigenstates with good quantum numbers are probed. Second, the restoration of symmetries and, in general, the use of configuration mixing techniques is a way to grasp some additional correlations associated with quantum fluctuations in a collective space [5,6]. Ultimately, the state of the art of the EDF approach is to perform a configuration mixing to describe the coexistence of different intrinsic configurations such as shapes, excited states, and electromagnetic and nuclear transitions.

This technique of symmetry breaking followed by symmetry restoration has been recently shown to lead to spurious contributions to the energy and must be applied with caution [7,8]. Overall, the very notion of symmetry breaking in a functional approach needs to be clarified [9]. For a detailed discussion, we refer the interested reader to the recent works of Refs. [7,8,10–13]. To face these difficulties, at present, three strategies have been proposed to perform well-converged configuration mixing calculations within the EDF approach: (i) Derive the energy functional starting from a true Hamiltonian and completely incorporate the Pauli principle [7]. (ii) Identify and remove spurious contributions from the energy functional [10–12]. This could be performed for some specific functionals, by comparing with the Hamiltonian case. (iii) Consistently extend the energy functional used in the SB case to a functional of the densities of the state with the symmetries restored. The latter strategy is the symmetry-conserving EDF (SC-EDF) approach proposed for the projection onto the good particle number in Ref. [14].

Strategies (i) and (ii) prevent us from using density-dependent interactions with noninteger powers of the density and strongly reduce our ability to tailor the density functional. Note that strategy (i) is nowadays used with the Gogny force [15–17], taking specific care of the density-dependent term. Recent applications of strategy (ii) have shown that this approach becomes rather involved when several symmetries are restored simultaneously [18]. While currently formulated only for the particle number restoration case (see also the discussion in Ref. [19]), strategy (iii) can be used for any functional form such as those used in the SB case starting from the Gogny or Skyrme-like interaction, while having a different interaction in the pairing channel. In addition, strictly enforcing antisymmetrization is not required and some useful numerical approximations such as the Slater approximation for the Coulomb exchange can be still used. In view of the recent discussion in [13], it should be stressed that the choice of density entering in the noninteger dependencies remains an open question. We take in this paper a conservative choice and use the projected density in such dependencies [15–17].

It is worth mentioning that, if a Hamiltonian is used as in strategy (i), the SC-EDF can always be formulated for all possible symmetry restorations. However, when different effective interactions are used in the mean-field and pairing channels, as is the case in most of the nuclear physics energy density functional applications, a careful analysis should be made to properly extend the SB functional. At present, this has been shown to be possible only for the particle number projection (PNP) by expressing the density in the canonical basis of the Bardeen-Cooper-Schrieffer (BCS)/Hartree-Fock-Bogoliubov (HFB) formalism, which is preserved during the projection [19]. The latter property will break down for any

*hupin1@llnl.gov
†lacroix@ganil.fr

 

other symmetry restoration. The problem of restoring other symmetries within the SC-EDF approach remains an open problem.

In this article, the work presented in Ref. [14] is extended to perform variation after projection (VAP), enforcing good particle number. We show that the SC-EDF used with the up-to-date functionals based on the Skyrme interaction can be competitive for describing pairing in nuclei.

## II. THE SYMMETRY-CONSERVING EDF APPROACH

By starting from a quasiparticle state $|\Phi_0\rangle$, the most currently used SB-EDF based on the Skyrme [20] or Gogny [21] forces can be written as

$$\mathcal{E}_{\rm SB}[\Phi_0] = \sum_i t_{ii}\rho_{ii} + \frac{1}{2}\sum_{i,j}\overline{v}^{\rho\rho}_{ijij}\rho_{ii}\rho_{jj} + \frac{1}{4}\sum_{i,j}\overline{v}^{\kappa\kappa}_{i\bar{i}j\bar{j}}\kappa^*_{i\bar{i}}\kappa_{j\bar{j}}, \tag{1}$$

where $\overline{v}^{\rho\rho}$ and $\overline{v}^{\kappa\kappa}$ denote the effective vertices in the particle-hole and particle-particle channels. Here $\rho$ and $\kappa$ denote the normal and anomalous densities expressed in the canonical basis.

In the Hamiltonian case, U(1) symmetry restoration can be performed by considering the component of the quasiparticle state with specific particle number. By introducing the particle number projector $P^N$, a new state $|\Psi_N\rangle$ can be defined through

$$|\Psi_N\rangle = P^N|\Phi_0\rangle. \tag{2}$$

While there is no ambiguity when a Hamiltonian is used, the main challenge within the EDF approach is to properly extend (1) to account for particle number conservation.

This problem has been carefully analyzed in Ref. [14], leading to a generalization of the energy density functional given by

$$\begin{aligned}\mathcal{E}_{\rm SC}[\hat{\rho}^N, \hat{R}^N] = &\sum_i t_{ii}\rho^N_{ii} + \frac{1}{2}\sum_{i\neq j, j\neq\bar{i}}\bar{v}^{\rho\rho}_{ijij}R^N_{jiji}\\ &+\frac{1}{2}\sum_i\left(\bar{v}^{\rho\rho}_{iiii}+\bar{v}^{\rho\rho}_{i\bar{i}i\bar{i}}\right)\left(\rho^N_{ii}\right)^2\\ &+\frac{1}{4}\sum_{i\neq j, i\neq\bar{j}}\bar{v}^{\kappa\kappa}_{i\bar{i}j\bar{j}}R^N_{j\bar{j}i\bar{i}}\\ &+\frac{1}{2}\sum_i\bar{v}^{\kappa\kappa}_{ii\bar{i}\bar{i}}\rho^N_{ii}\left(1-\rho^N_{ii}\right),\end{aligned} \tag{3}$$

where $\rho^N$ and $R^N$ denote, respectively, the one- and two-body matrices of the projected state, Eq. (2). Note that it is further postulated that any dependence of the effective vertices in terms of the SB density should be replaced by an equivalent dependence of the projected density. By doing so, the energy becomes a functional of the projected state degrees of freedom (DOF) only. Note that, for other symmetries [13], this assumption leads to serious difficulties and remains an open question. In former applications of SC-EDF, the expression of the energy has been used in the projection after variation (PAV) scheme, showing the absence of any pathologies previously observed, even if density-dependent interactions are used in the functional.

Here, the SC-EDF is applied to perform VAP. In this case, the energy should be minimized with respect to all possible variations of the projected state DOF, i.e.,

$$\delta\mathcal{E}_{\rm SC}[\hat{\rho}^N, \hat{R}^N] = 0. \tag{4}$$

In the following we will consider the specific case where the state $|\Phi_0\rangle$ is written in a BCS form as

$$|\Phi_0\rangle = \prod_{i>0}(u_i + v_i a^\dagger_i a^\dagger_{\bar{i}})|0\rangle, \tag{5}$$

with $u_i^2 + v_i^2 = 1$. Accordingly, variation of the projected state DOF can be recast into variations of the single-particle state components $\phi_i(\mathbf{r})$ associated with the creation operator $a^\dagger_i$ and variations of the quantity $v_i^2$ corresponding to the SB occupancy of orbital $i$. We then end up with a set of coupled equation to be solved self-consistently:

$$\frac{\delta\mathcal{E}_{\rm SC}}{\partial\phi^\star_i(\mathbf{r})} = 0, \quad \frac{\delta\mathcal{E}_{\rm SC}}{\partial v_i^2} = 0. \tag{6}$$

This procedure is the same as the one generally used in the Hamiltonian case in PNP-VAP [22–24]. The eigenvalue equations of the self-consistent problem are recalled and explained in the Appendix. It is worth mentioning that we took advantage of the analytic expressions of the densities $R^N$ [25]. This step is crucial to reduce the computational burden of the calculation.

The Euler-Lagrange equations associated with the minimization of the energy yield a set of eigenvalues and nonlinear equations that are rather involved numerically. As explained in the Appendix, each single-particle state evolves with its own potential. This increases the numerical cost of the approach. By taking advantage of the EDF flexibility without breaking the consistency requirement, the minimization can be greatly simplified numerically by making the assumption in Eq. (3) that

$$R^N_{jiji} \simeq \rho^N_{ii}\rho^N_{jj}. \tag{7}$$

With this approximation, the usual picture of single-particle states evolving with the same mean field is recovered. To quantify the effect of approximation (7), PAV has been performed either using directly $R^N_{jiji}$ or using its approximate form. An illustration of the results is shown in Fig. 1 for a tin isotope in the mid-shell as a function of deformation. It can be seen in this figure that the total energy is slightly lower when approximation (7) is made while the shape of the energy landscape is globally unchanged. It should be noted that, following the spirit of density functional theory, such a shift can easily be compensated by readjusting the functional parameters. It is clear that the use of the complete two-body matrix elements is desirable, but approximation (7) greatly improves the convergence of the minimization while leading to nonzero pairing even close to magicity. This approximation, which appears as a compromise between practical constraints and the improvement of pairing, is used in the following.

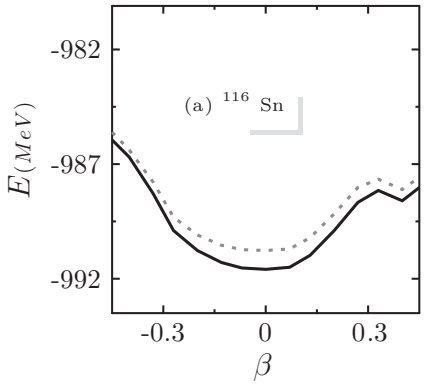


FIG. 1. Evolution of the total energy given by the full SC-EDF functional (gray dotted line) and using the approximation of Eq. (7) (black solid line) at the PAV level as a function of the deformation of the $^{116}$Sn nucleus.

## III. APPLICATIONS

The EV8 code of Bonche, Flocard, and Heenen [26] has been updated to allow minimization of the functional (3) using the approximation in Eq. (7). The numerical method consists in solving the mean-field problem by using an imaginary time-step method [27] and the optimization of the occupation probabilities by using sequential quadratic programming. In the following, the SC-EDF method is used with the SLy4 interaction in the mean-field channel [28] while the effective pairing interaction considered [29] is

$$v^{\kappa\kappa}(\mathbf{r},\mathbf{r}') = \frac{V_0}{2}(1-P_\sigma)\left[1-\left(\frac{\rho(\mathbf{R})}{\rho_0}\right)^{\alpha}\right]\delta(\mathbf{r}-\mathbf{r}'), \qquad (8)$$

with $\mathbf{R} = (\mathbf{r}+\mathbf{r}')/2$. $V_0 = 1250$ MeV is the pairing constant, $\alpha = 1$, and $\rho_0 = 0.16$ fm$^{-3}$ is the saturation density. In addition, to avoid the ultraviolet divergence that appears with contact interaction, a cutoff factor [30] with an energy interval of 5 MeV is used to select states around the Fermi energy. These values have been typically used to reproduce neutron and proton separation energies [31] and, in the standard terminology, correspond to a surface pairing.

In this work, SC-EDF calculations are systematically performed for the Kr and Sn isotopic chains. In the latter case, the proton number is magic while in the former case it is not. As an illustration of the results, the evolution of the energy as a function of the deformation obtained with the SC functional (blue solid line) is compared to the original BCS result (green dashed line) for $^{72}$Kr and $^{86}$Kr, respectively, in Figs. 2(a) and 2(b). Similar curves are shown in Fig. 3 for $^{116}$Sn and $^{132}$Sn. These nuclei have been selected because they are representative of the different types of situations: a mid-shell nucleus ($^{72}$Kr), simply magic nuclei ($^{86}$Kr and $^{116}$Sn), or a doubly magic nucleus ($^{132}$Sn). The results have been obtained by adding a quadrupole constraint in the minimization while the deformation parameter is defined by

$$\beta = \sqrt{\frac{5}{16\pi}}\frac{4\pi}{3R^2A}\langle Q_{20}\rangle, \qquad (9)$$

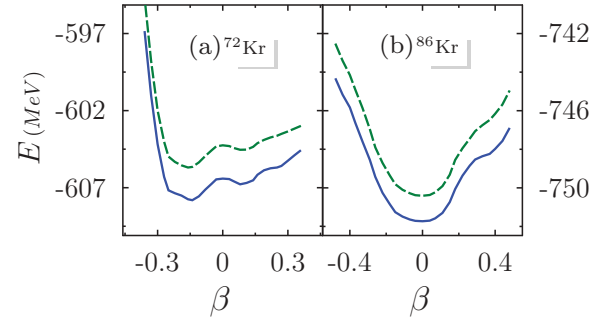


FIG. 2. (Color online) Evolution of the energy obtained using the VAP calculation (blue solid line) for (a) $^{72}$Kr and (b) $^{86}$Kr as a function of deformation. In each case, the BCS result obtained with the original EV8 code is shown with a green dashed curve.

where $\langle Q_{20}\rangle$ is the quadrupole deformation and $R = 1.2A^{1/3}$ is the nuclear radius. It can be seen in Figs. 2 and 3 that the potential energy curves obtained with the SC-EDF are smooth.

As already discussed in Ref. [14], no additional pathologies in the projection with density-dependent interactions [8,11] are expected. This stems from the fact that the projected densities are used to calculate the energy; nevertheless, the functional is subject to the same problems as the original symmetry-breaking EDF (for instance, possible self-interaction).

Figures 2 and 3 illustrate that the energy potential curves of the SC-EDF with respect to the quadrupole deformation are shifted from those of the BCS formalism. There are no changes in the shape of these curves, both the BCS and the shifted SC functionals can be almost superimposed. The energy gain, illustrated by the shift, is between 1 and 2 MeV for mid-shell and simply magic nuclei while the doubly magic nuclei $^{132}$Sn gains more than 0.5 MeV. This increase in correlation energy comes from the improved treatment of the pairing correlations from the projection formalism that has been used to tailor the functional dependancies of the energy.

As seen from Figs. 2 and 3, the full SC functional induces rather small differences on the total energy compared to the original BCS case. It should be mentioned, however, that the pairing energy is always enhanced when the symmetry is conserved, especially around shell closures, as expected. Indeed, when the pairing is treated within BCS or HFB formalisms, there is a sudden disappearance of correlations in the weak-pairing regime. This is the known as the BCS threshold anomaly. A measure of the pairing strength is

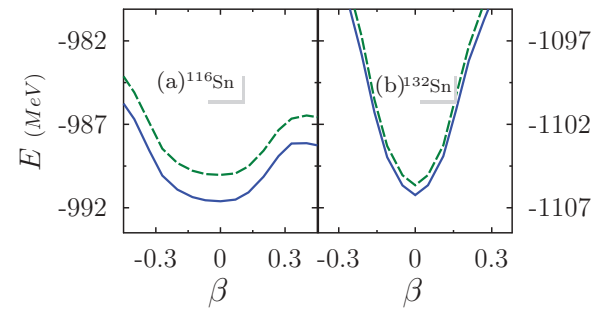


FIG. 3. (Color online) Same as Fig. 2 for (a) $^{116}$Sn and (b) $^{132}$Sn.

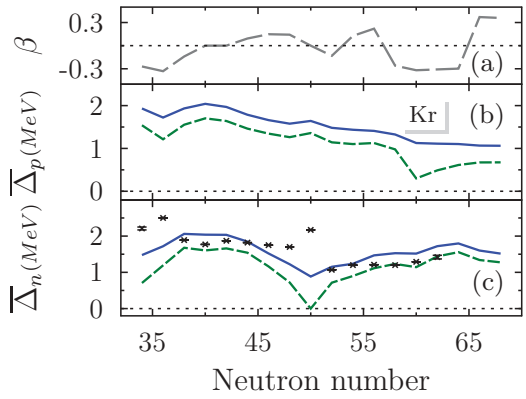


FIG. 4. (Color online) Value of the deformation parameter $\beta$ [Eq. (9)] at (a) the minimum, (b) average proton, and (c) neutron mean gaps defined by Eq. (10) shown as a function of the neutron number along the Kr isotopic chain obtained from BCS (green dashed lines) and the SC-EDF (blue solid lines) approaches. The deformation parameter at the minimum is the same for both BCS and SC-EDF (gray long dashed line) cases. The calculations are performed with a SLy4 effective interaction that includes a noninteger density dependence and a density-dependent pairing interaction [Eq. (8)]. The minimization is performed including the quadrupole degree of freedom. In the neutron case, the experimental gaps (black crosses) and their error bars [34] obtained with the three-point formula (see [32,33]) are also presented.

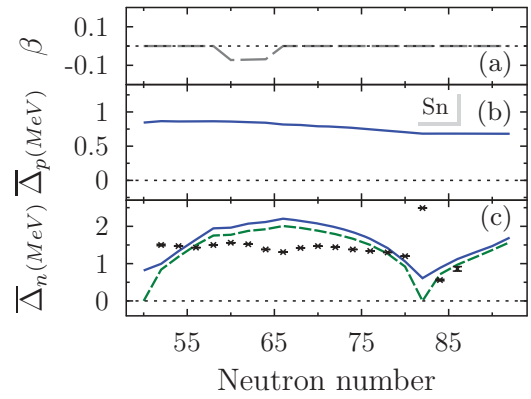


FIG. 5. (Color online) Same as Fig. 4 for the Sn isotopic chain. The proton mean gap (b) for the BCS case is identified with zero along the isotopic line.

provided by the mean gap [32]

$$\overline{\Delta}_{n/p} = \frac{E^{n/p}_{\text{pairing}}}{\sum_i \sqrt{\rho_{ii}(1-\rho_{ii})}}, \tag{10}$$

where $\rho_{ii}$ are the occupation probabilities of a given theory and $E^{n/p}_{\text{pairing}}$ is the neutron-proton pairing energy. In the SC-EDF formalism, these energies are calculated as the sum of the last two terms in Eq. (3). This observable has the advantages of (i) correlating with the pairing gap in the limit of a constant pairing interaction and (ii) probing both the pairing energy and the trend of the occupation probabilities, such as the fragmentation of occupation numbers around the Fermi surface.

In Figs. 4 and 5, the deformation parameter $\beta$ [Eq. (9)] at the minimum of the energy [Figs. 4(a) and 5(a)] and the average proton [Figs. 4(b) and 5(b)] and neutron [Figs. 4(c) and 5(c)] gaps are shown as a function of the neutron number along the Kr and Sn isotopic chains, respectively. The BCS (green dashed lines) and the SC-EDF (blue solid lines) results are compared. Note that consistently with the observations from Figs. 2 and 3, the deformation parameter at the minimum of the energy (long dashed line) is the same for both BCS and SC-EDF cases (and hence is plotted once). In this figure, the BCS case exhibits strong variations of the gap near the $N = 50$ shell closure. This is a fingerprint of the abrupt disappearance of pairing in this formalism close to magicity. It is also worth keeping in mind that the evolution of deformation as $N$ increases might also induce local fluctuations. This is the case for $N > 56$ in the Kr chain, as we can see from the evolution of the deformation [Fig. 4(a)] reflected by variations in Figs. 4(b) and 4(c).

In the SC-EDF case, it is observed that the pairing gap is systematically enhanced compared to the BCS results. This enhancement is increased at the shell closure. For instance, in the proton gap of Sn isotopes, a mean gap of $\sim 0.7$ MeV is obtained (see Fig. 5), compared to zero MeV at the BCS level. In the Kr isotopic chain, both BCS and SC-EDF approaches lead to deformed nuclei with the same deformation parameter. The increase of pairing correlations is only due to a better treatment of quantum fluctuations in gauge space by the SC method. It is then seen that the increase at the shell closure ($N = 50$) is further enhanced to $\sim 1$ MeV, while it is of the order of 0.3–0.5 MeV in the mid-shell. Altogether, the pairing gap obtained within the VAP approach is much smoother than the BCS pairing gap and more consistent with experimental observations.

It is important to note that the increase of the pairing gap is not fully reflected in the lowering of the ground-state binding energy. Indeed, the SC-EDF approach is fully self-consistent and, when the enhanced pairing is built up in the minimization, the mean field reorganizes. Generally, it is observed that the mean-field energy, denoted by $E_{\text{MF}}$ and defined as the total energy minus the pairing energy, increases slightly and partially compensates for the effect of the pairing. In Figs. 6 and 7, the three quantities

$$\Delta E_{\text{pairing}} = E^{\text{VAP}}_{\text{pairing}} - E^{\text{BCS}}_{\text{pairing}},$$
$$\Delta E_{\text{MF}} = E^{\text{VAP}}_{\text{MF}} - E^{\text{BCS}}_{\text{MF}},$$

and

$$\Delta E_{\text{tot}} = E^{\text{VAP}}_{\text{tot}} - E^{\text{BCS}}_{\text{tot}}$$

are displayed as a function of the neutron number, respectively, from panels (a) to (c) for the Kr and Sn isotopes. In these figure, we see that $\Delta E_{\text{pairing}}$ [Figs. 6(a) and 7(a)] is always negative while $\Delta E_{\text{MF}}$ [Figs. 6(b) and 7(b)] is always positive and, therefore, the net reduction of the total energy [Figs. 6(c) and 7(c)] is much less than the pairing correlation would suggest. Altogether, the total energy is shifted. The transition from a sharp Fermi distribution around single or doubly magic nuclei with the BCS approach to a fragmented Fermi surface with nonzero pairing within the SC-EDF approach leads to a significant change in the mean-field energy, especially due

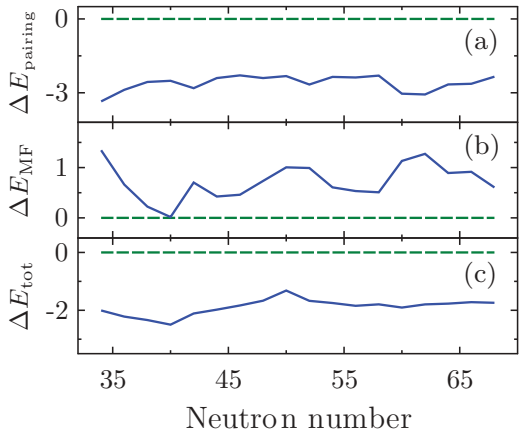


FIG. 6. (Color online) Evolution of the quantities $\Delta E_{\rm pairing}$ (a), $\Delta E_{\rm MF}$ (b), and $\Delta E_{\rm tot}$ (c) along the Kr isotopic chain. The horizontal dashed line corresponds to the case where BCS and SC-EDF results would be identical. The vertical axis has units of MeV.

to the contribution of single-particle levels above the Fermi energy. We can observe this effect in both Figs. 6 and 7. However, it is not possible to give more general trends because of the deformation and self-consistency of the theory.

In Fig. 8, the two-neutron separation energies $S_{2n}$ obtained in the BCS (green dashed line) and SC-EDF (blue solid line) approaches are compared with experimental values (black open circles). This quantity is sometime used in the literature to adjust the pairing effective interaction parameters. Both BCS and VAP results are consistent with experiment. In fact, the $S_{2n}$ value are not affected by the variation after projection performed within the SC-EDF formalism.

The applications of the SC-EDF show that the bulk properties (Figs. 2, 3, and 8) of the underlying effective interaction are conserved while the total binding and pairing energies are shifted (Figs. 6 and 7). For all nuclei studied here, the SC-EDF predicts a nonzero pairing energy and a fragmented Fermi surface. This is reflected by the nonzero pairing gap (Figs. 4 and 5) for all nuclei, including single and doubly magic ones where the BCS approach leads to a Fermi distribution for the orbital occupancies. In the following,

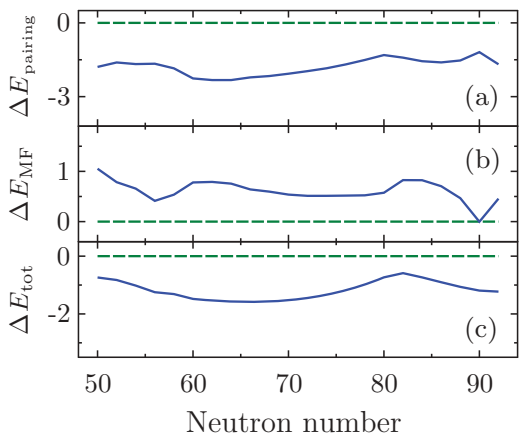


FIG. 7. (Color online) Same as Fig. 6 for the Sn isotopic chain. The vertical axis has units of MeV.

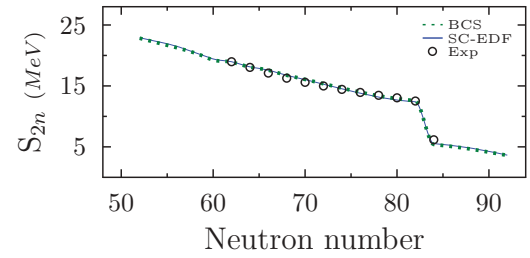


FIG. 8. (Color online) Comparison of the two neutron separation energies $S_{2n}$ along the Sn isotopic chain between BCS (green dotted line) and SC-EDF (blue solid line) approaches with the experimental values (black open circles).

the evolution of these observations are investigated in a brief discussion as a function of the refitting of the strength $V_0$ of the pairing interaction.

## IV. DISCUSSION OF THE PAIRING STRENGTH

The pairing interaction used above is often adjusted to properly describe pairing gaps in the EDF approach using BCS or HFB formalisms especially in the mid-shell [32,35–37]. It is known in the literature [2] that one should *a priori* readjust the pairing strength when the functional changes. In this section, the results of VAP with an optimal value of the pairing strength are presented.

In Figs. 9 and 10, results of the BCS (green dashed line) and SC-EDF (blue solid line) approaches with a pairing strength $V_0 = 1100$ MeV are shown. This value of the strength has been chosen to properly describe Kr isotopes in the open shell and agrees with previous studies (see for instance [38]). By comparing these figures with Figs. 4 and 5, it can be observed that the SC-EDF with the reduced pairing interaction reproduces the original BCS result (with $V_0 = 1250$ MeV) in open-shell nuclei.

Refitting of the pairing interaction solely when incorporating particle number projection is too simplistic a strategy to properly describe both the pairing and the bulk properties in nuclei. To improve the quality of theories that go beyond the mean field by restoring symmetries, it is anticipated that

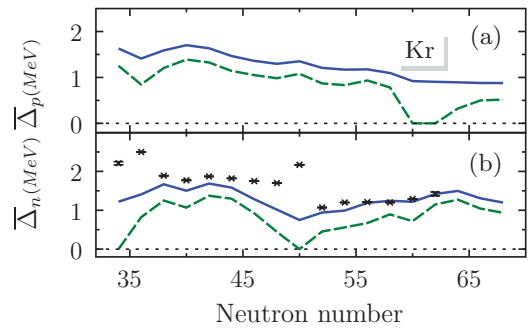


FIG. 9. (Color online) Same as Fig. 4 with a pairing strength of $V_0 = 1100$ MeV. The green dashed curve corresponds to the BCS result while the blue solid line corresponds to the SC-EDF case.

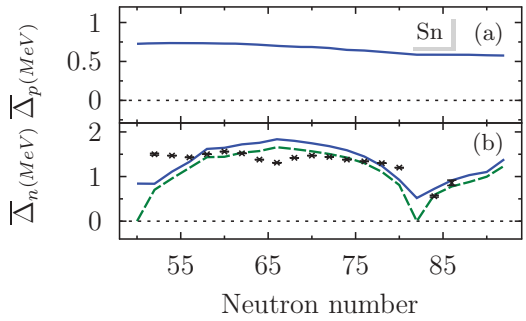


FIG. 10. (Color online) Same as Fig. 5 for the Sn isotopes.

a complete readjustment of all components of the functional (mean-field and pairing) has to be performed.

## V. CONCLUSION

The recently proposed symmetry-conserving EDF approach that incorporates the effect of particle number conservation is used in the variation after projection scheme. The VAP is applied using density-dependent interactions in both the mean-field and pairing channels. Such a density dependence, while impossible to use in configuration mixing calculations, does not lead to any difficulty in the SC-EDF framework. The particle-hole functional is simplified to allow a more efficient treatment and illustrates that the pairing energy of the SC-EDF yields an improved description of pairing correlations. A systematic study of the krypton and tin isotopic chains is made, showing the increase of pairing energy when particle number conservation is taken into account self-consistently. In particular, the description of correlations in the vicinity of closed-shell nuclei is improved. Indeed, as expected, the symmetry-conserving theory predicts nonvanishing pairing gaps around and at shell closures. The present study clearly shows that the incorporation of symmetry restoration leads to an enriched functional. Here, we reduce the pairing strength in order to properly describe pairing gaps. We recall that, ultimately, coefficients of the functional in both mean-field and pairing channels should be simultaneously optimized to really improve the predictive power using EDF approaches.

## ACKNOWLEDGMENT

This work in part is performed under the auspices of the US Department of Energy by Lawrence Livermore National Laboratory under Contract No. DE-AC52-07NA27344.

## APPENDIX: EULER-LAGRANGE EQUATIONS

In the case of the SC-EDF built from a quasiparticle vacuum and a two-body delta interaction, the eigenequations to be solved as a self-consistent mean-field problem read

$$\frac{\partial \mathcal{E}_{\rm SC}}{\partial \phi_i^\star(\mathbf{r})} = \Bigg(-\frac{\hbar^2}{2m}\Delta + \sum_{j\neq(i,\bar{i})} \frac{\partial \bar{v}^{\rho\rho}_{ijij}}{\partial \phi_i^\star(\mathbf{r})\partial\phi_i(\mathbf{r})}\frac{R^N_{jiji}}{\rho^N_{ii}} + \frac{\partial \bar{v}^{\rho\rho}_{iiii}}{\partial \phi_i^\star(\mathbf{r})\partial\phi_i(\mathbf{r})}\rho^N_{ii} - \varepsilon_i\Bigg)\rho^N_{ii}\phi_i(\mathbf{r}), \quad \text{(A1)}$$

where the contribution from the pairing part of the functional has been neglected as is usually done, $\bar{v}^{\rho\rho}$ is a particle-hole contact interaction, $R^N_{jiji}$ is the projection of the one-body density acting in the particle-hole channel, and $\varepsilon_i$ is the Lagrange multiplier that enforces the normalization of the single-particle state $\phi_i$. It can be noted that in this form there is one potential for each orbital due to the density dependence in the summation. The role of the prescription in Eq. (7) is to remove this dependency, hence recovering a single mean-field for all orbits.

[1] M. Bender, P.-H. Heenen, and P.-G. Reinhard, Rev. Mod. Phys. **75**, 121 (2003).
[2] P. Ring and P. Schuck, *The Nuclear Many-Body Problem* (Springer-Verlag, Berlin, 1980).
[3] P.-G. Reinhard, Nucl. Phys. A **420**, 173 (1984).
[4] W. Nazarewicz, Prog. Part. Nucl. Phys. **28**, 307 (1992).
[5] J. L. Egido and P. Ring, Nucl. Phys. A **383**, 189 (1982).
[6] J. L. Egido and P. Ring, Nucl. Phys. A **388**, 19 (1982).
[7] M. Anguiano, J. L. Egido, and L. M. Robledo, Nucl. Phys. A **696**, 467 (2001).
[8] J. Dobaczewski, M. V. Stoitsov, W. Nazarewicz, and P.-G. Reinhard, Phys. Rev. C **76**, 054315 (2007).
[9] T. Duguet and J. Sadoudi, J. Phys. G **37**, 064009 (2010).
[10] M. Bender, T. Duguet, and D. Lacroix, Phys. Rev. C **79**, 044319 (2009).
[11] T. Duguet, M. Bender, K. Bennaceur, D. Lacroix, and T. Lesinski, Phys. Rev. C **79**, 044320 (2009).
[12] D. Lacroix, T. Duguet, and M. Bender, Phys. Rev. C **79**, 044318 (2009).
[13] L. M. Robledo, J. Phys. G **37**, 064020 (2010).
[14] G. Hupin, D. Lacroix, and M. Bender, Phys. Rev. C **84**, 014309 (2011).
[15] N. López Vaquero, T. R. Rodriguez, and J. L. Egido, Phys. Lett. B **704**, 520 (2011); **705**, 543 (2011).
[16] T. R. Rodríguez and J. L. Egido, Phys. Rev. Lett. **99**, 062501 (2007).
[17] T. R. Rodríguez and J. L. Egido, Phys. Rev. C **81**, 064323 (2010).
[18] M. Bender *et al*. (private communication).
[19] G. Hupin and D. Lacroix, Prog. Theor. Phys. Suppl. (to be published), arXiv:1203.3925.
[20] T. H. R. Skyrme, Nucl. Phys. **9**, 615 (1959).
[21] D. Gogny, P. Pires, and D. R. Tourreil, Phys. Lett. B **32**, 591 (1970).
[22] J. A. Sheikh and P. Ring, Nucl. Phys. A **665**, 71 (2000).
[23] J. A. Sheikh, E. Lopes, and P. Ring, Phys. At. Nucl. **64**, 477 (2001).
[24] K. Dietrich, H. J. Mang, and J. H. Pradal, Phys. Rev. **135**, B22 (1964).
[25] D. Lacroix and G. Hupin, Phys. Rev. B **82**, 144509 (2010).
[26] P. Bonche, H. Flocard, and P.-H. Heenen, Comput. Phys. Commun. **171**, 49 (2005).

[27] K. T. R. Davies, H. Flocard, S. J. Krieger, and M. S. Weiss, Nucl. Phys. A **342**, 111 (1980).
[28] E. Chabanat, P. Bonche, P. Haensel, J. Meyer, and R. Schaeffer, Nucl. Phys. A **635**, 231 (1998).
[29] R. R. Chasman, Phys. Rev. C **14**, 1935 (1976).
[30] P. Bonche, H. Flocard, P.-H. Heenen, S. J. Krieger, and M. S. Weiss, Nuc. Phys. A **443**, 3963 (1985).
[31] C. Rigollet, P. Bonche, H. Flocard, and P.-H. Heenen, Phys. Rev. C **59**, 3120 (1999).
[32] J. Dobaczewski, H. Flocard, and J. Treiner, Nucl. Phys. A **422**, 103 (1984).
[33] T. Duguet, P. Bonche, P.-H. Heenen, and J. Meyer, Phys. Rev. C **65**, 014311 (2001).
[34] Data retrieved from the National Nuclear Data Center database, version of 03/04/2012, Online Data Service.
[35] J. Dobaczewski, W. Nazarewicz, and T. R. Werner, Phys. Scr. T **56**, 15 (1995).
[36] T. Lesinski, K. Bennaceur, T. Duguet, and J. Meyer, Phys. Rev. C **74**, 044315 (2006).
[37] J. Margueron, H. Sagawa, and K. Hagino, Phys. Rev. C **76**, 064316 (2007).
[38] A. Valor, P.-H. Heenen, and P. Bonche, Nuc. Phys. A **671**, 145 (2000).